EXOTIC CHARACTERISTICS OF POWER PROPAGATION IN THE CHIRAL NIHILITY FIBER

J. Dong

Institute of Optical Fiber Communication and Network Technology
Ningbo University
Ningbo 315211, China

Abstract—The novel characteristics of power propagation of guided modes in the chiral nihility fiber have been investigated theoretically. The formulas of electromagnetic fields in the core and cladding for guided modes are presented in detail. The dispersion equations, energy flux and power of guided modes are derived. The numerical results are given and discussed. Some exotic features of power propagation have been found in the chiral nihility fiber.

1. INTRODUCTION

During the last decade, much interest has been focused on the negative index material (NIM, also called left-handed material (LHM) or double negative (DNG) metamaterial) [1–6]. NIM has many unique features [7] and fascinating potential applications such as perfect lens [8], cloaking [9], slow light [10], and novel devices [11, 12]. Various NIM waveguides, including the slab [13–16], grounded slab [17–19], and circular [20–24] waveguides filled with NIMs in the core or cladding, have been investigated intensively. Many novel characteristics of electromagnetic waves in NIM waveguides were found. For example, surface mode, mode double or three degeneracy, and sign-varying energy flux [14], slow wave propagation, even 'trapped rainbow' effect [10].

Recently, theoretical and experimental studies have shown that chiral metamaterials can achieve negative refractive index (NRI) because of its chirality [25–36]. NRI chiral metamaterials can also be used as a "perfect lens", but for circularly polarized waves [29, 30]. The unusual characteristics of guided and surface modes in chiral

---

Corresponding author: J. Dong (dongjianfeng@nbu.edu.cn).

negative refraction slab [37, 38], grounded slab [39] and parallel-plate waveguides [40] have been investigated theoretically. Chiral nihility metamaterial is a special case of chiral negative refraction medium, in which the permittivity and permeability are simultaneously zero [25, 41]. Waves in the chiral nihility metamaterial waveguides have also been examined in literature [42–45] and our previous papers [46, 47]. Although chiral fibers have been investigated during the last two decades due to their potential applications in optical communications, optical sensors and integrated optics devices [48–51], chiral nihility fiber has not been studied yet. In our previous work [52], we have investigated the effect of chiral parameter on dispersion curves of guided and surface modes in the chiral nihility fiber. In this paper, we focus on the characteristics of power propagation of guided modes in the chiral nihility fiber. We present the formulas of electromagnetic fields in the core and cladding for guided modes in detail, and then the dispersion equations, energy flux and power of guided modes are obtained. Numerical results are given and discussed. Some exotic features have been found in the chiral nihility fiber.

2. FORMULATIONS

Consider the chiral nihility fiber whose geometry and material parameters are shown in Fig. 1. The core is isotropic chiral nihility metamaterial, $\varepsilon_1 = 0$, $\mu_1 = 0$, $\kappa \neq 0$, and the cladding is conventional dielectric material ε_2, μ_2. The radius of core is a. The cladding is assumed to extend infinitely. Here we adopt cylindrical coordinate system (r, φ, z).

The constitutive relations in an isotropic chiral medium for a time-
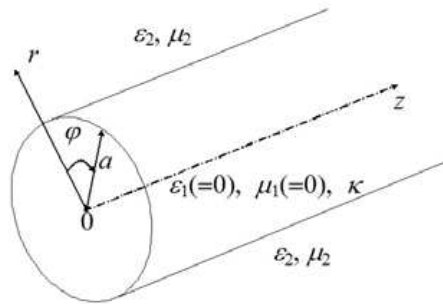
Figure 1. Geometry and material parameters of the chiral nihility fiber.

harmonic field with $\exp(j\omega t)$ are as follows [27]:

$$\mathbf{D} = \varepsilon\mathbf{E} - j\kappa\sqrt{\mu_0\varepsilon_0}\mathbf{H}, \quad \mathbf{B} = \mu\mathbf{H} + j\kappa\sqrt{\mu_0\varepsilon_0}\mathbf{E} \tag{1}$$

where μ, ε, κ are the permeability, permittivity and chirality parameter of the chiral medium, respectively. Chiral nihility metamaterial is a special case of chiral medium, in which the permittivity and permeability are simultaneously zero at certain frequency, i.e., $\varepsilon = 0$, $\mu = 0$, $\kappa \neq 0$, and the constitutive relations reduce to [25]:

$$\mathbf{D} = -j\kappa\sqrt{\mu_0\varepsilon_0}\mathbf{H}, \quad \mathbf{B} = j\kappa\sqrt{\mu_0\varepsilon_0}\mathbf{E} \tag{2}$$

In the chiral nihility metamaterial, there exist right-handed (RCP, +) and left-handed (LCP, −) circularly polarized eigenwaves, whose wavenumbers are $k_\pm = \pm\kappa k_0$.

The electromagnetic fields in the chiral nihility metamaterial can be decomposed as [27]:

$$\mathbf{E} = \mathbf{E}_+ + \mathbf{E}_-, \quad \mathbf{H} = \frac{j}{\eta}(\mathbf{E}_+ - \mathbf{E}_-) \tag{3}$$

where $\eta = \lim\limits_{\mu\to 0,\varepsilon\to 0}\sqrt{\mu/\varepsilon}$ is the wave impedance of the chiral nihility metamaterial. It has been shown that $\mathbf{E}_\pm$ satisfy following equations:

$$\nabla \times \mathbf{E}_\pm = \pm k_\pm\mathbf{E}_\pm \tag{4}$$

By separating $\mathbf{E}_\pm$ into transversal $\mathbf{E}_{\pm t}$ and longitudinal $E_{\pm z}$ components, we obtain

$$\mathbf{E}_\pm = \mathbf{E}_{\pm t} + \hat{\mathbf{z}}E_z \tag{5}$$

The relationship between the transversal and longitudinal electromagnetic field components can be derived from Equation (4):

$$\mathbf{E}_{\pm t} = \frac{1}{\kappa^2 k_0^2 - \beta^2}\left[-j\beta\nabla_t E_{\pm z} - \kappa k_0\hat{\mathbf{z}} \times \nabla_t E_{\pm z}\right] \tag{6}$$

where $\nabla_t = \nabla - \hat{\mathbf{z}}\frac{\partial}{\partial z}$, z dependence is known as $\exp(-j\beta z)$ and omitted for simplicity, and β is the longitudinal propagation constant. In the cylindrical coordinate system (r, φ, z), the transversal electromagnetic field components can be expressed as:

$$\begin{pmatrix} E_r \\ H_r \\ E_\varphi \\ H_\varphi \end{pmatrix} = \begin{pmatrix} \frac{-j\beta}{k_{r+}^2} & \frac{k_+}{k_{r+}^2} & \frac{-j\beta}{k_{r-}^2} & \frac{-k_-}{k_{r-}^2} \\ \frac{\beta}{\eta k_{r+}^2} & \frac{jk_+}{\eta k_{r+}^2} & \frac{-\beta}{\eta k_{r-}^2} & \frac{jk_-}{\eta k_{r-}^2} \\ \frac{-k_+}{k_{r+}^2} & \frac{-j\beta}{k_{r+}^2} & \frac{k_-}{k_{r-}^2} & \frac{-j\beta}{k_{r-}^2} \\ \frac{-jk_+}{\eta k_{r+}^2} & \frac{\beta}{\eta k_{r+}^2} & \frac{-jk_-}{\eta k_{r-}^2} & \frac{-\beta}{\eta k_{r-}^2} \end{pmatrix} \begin{pmatrix} \frac{\partial}{\partial r}E_{+z} \\ \frac{\partial}{r\partial\varphi}E_{+z} \\ \frac{\partial}{\partial r}E_{-z} \\ \frac{\partial}{r\partial\varphi}E_{-z} \end{pmatrix} \tag{7}$$

From Equation (4), wave equations of $\mathbf{E}_\pm$ can be obtained as:

$$\left(\nabla^2 + k_\pm^2\right)\mathbf{E}_\pm = 0 \tag{8}$$

In the chiral nihility fiber core, the longitudinal components of the electromagnetic fields $\mathbf{E}_\pm$ can be written as:

$$\begin{cases} E_{+z1} = A_m J_m\left(k_{r+}r\right)\exp(jm\varphi) \\ E_{-z1} = B_m J_m\left(k_{r-}r\right)\exp(jm\varphi) \end{cases} \tag{9}$$

where A_m, B_m are constants, $J_m(\cdot)$ is the Bessel function of first kind, m is a positive and negative integer specifying the azimuthal field dependence, $k_{r\pm} = \sqrt{k_\pm^2 - \beta^2} = k_0\sqrt{\kappa^2 - (\beta/k_0)^2} = k_r$ are the transverse wavenumbers of RCP and LCP eigenwaves in the core. k_r is a real number for guided mode ($\beta < \kappa k_0$) and an imaginary number for surface mode ($\beta > \kappa k_0$) [52].

Thus, from Equations (3) and (7), in the chiral nihility fiber core, the electromagnetic fields can be obtained as:

$$\begin{cases} E_{r1} = (A_m + B_m)\left[\frac{jm\kappa k_0}{k_r^2 r}J_m\left(k_r r\right) - \frac{j\beta}{k_r}J_m'\left(k_r r\right)\right]\exp(jm\varphi) \\ H_{r1} = \frac{j}{\eta_1}(A_m - B_m)\left[\frac{jm\kappa k_0}{k_r^2 r}J_m\left(k_r r\right) - \frac{j\beta}{k_r}J_m'\left(k_r r\right)\right]\exp(jm\varphi) \end{cases} \tag{10a}$$

$$\begin{cases} E_{\varphi 1} = (A_m + B_m)\left[\frac{\beta m}{k_r^2 r}J_m\left(k_r r\right) - \frac{\kappa k_0}{k_r}J_m'\left(k_r r\right)\right]\exp(jm\varphi) \\ H_{\varphi 1} = \frac{j}{\eta_1}(A_m - B_m)\left[\frac{\beta m}{k_r^2 r}J_m\left(k_r r\right) - \frac{\kappa k_0}{k_r}J_m'\left(k_r r\right)\right]\exp(jm\varphi) \end{cases} \tag{10b}$$

$$\begin{cases} E_{z1} = (A_m + B_m) J_m\left(k_r r\right)\exp(jm\varphi) \\ H_{z1} = \frac{j}{\eta_1}(A_m - B_m) J_m\left(k_r r\right)\exp(jm\varphi) \end{cases} \tag{10c}$$

where $\eta_1 = \lim\limits_{\mu_1 \to 0, \varepsilon_1 \to 0}\sqrt{\mu_1/\varepsilon_1}$ is the wave impedance in the core, $J_m'(\cdot)$ stands for differentiation with respect to argument.

Accordingly, in the cladding, the electromagnetic fields can be obtained as:

$$\begin{cases} E_{r2} = \left[(C_m - D_m)\frac{-jmk_2}{\tau_2^2 r}K_m\left(\tau_2 r\right) + (C_m + D_m)\frac{j\beta}{\tau_2}K_m'\left(\tau_2 r\right)\right] \\ \quad \exp(jm\varphi) \\ H_{r2} = \frac{j}{\eta_2}\left[(C_m + D_m)\frac{-jmk_2}{\tau_2^2 r}K_m\left(\tau_2 r\right) + (C_m - D_m)\frac{j\beta}{\tau_2}K_m'\left(\tau_2 r\right)\right] \\ \quad \exp(jm\varphi) \end{cases} \tag{11a}$$

$$\begin{cases} E_{\varphi 2} = \left[(C_m + D_m)\frac{-m\beta}{\tau_2^2 r}K_m\left(\tau_2 r\right) + (C_m - D_m)\frac{k_2}{\tau_2}K_m'\left(\tau_2 r\right)\right] \\ \quad \exp(jm\varphi) \\ H_{\varphi 2} = \frac{j}{\eta_2}\left[(C_m - D_m)\frac{-m\beta}{\tau_2^2 r}K_m\left(\tau_2 r\right) + (C_m + D_m)\frac{k_2}{\tau_2}K_m'\left(\tau_2 r\right)\right] \\ \quad \exp(jm\varphi) \end{cases} \tag{11b}$$

$$\begin{cases} E_{z2} = (C_m + D_m) K_m\left(\tau_2 r\right)\exp(jm\varphi) \\ H_{z2} = \frac{j}{\eta_2}(C_m - D_m) K_m\left(\tau_2 r\right)\exp(jm\varphi) \end{cases} \tag{11c}$$

where C_m, D_m are constants, $K_m(\cdot)$ is the modified Bessel function of second kind and $K'_m(\cdot)$ stands for differentiation with respect to argument, $\tau_2 = k_0\sqrt{(\beta/k_0)^2 - n_2^2}$ is the transverse attenuation factor in the cladding; $k_2 = \omega\sqrt{\mu_2\varepsilon_2}$, $\eta_2 = \sqrt{\mu_2/\varepsilon_2}$ are the wavenumber and wave impedance in the cladding, respectively.

According to four boundary conditions (continuity of the tangential electromagnetic field components E_z, E_φ, H_z, H_φ) at $r = a$, the dispersion equations of guided modes can be derived as:

$$\frac{m\beta}{a}\left(\frac{1}{k_r^2} + \frac{1}{\tau_2^2}\right) - \frac{\kappa k_0}{k_r}\hat{J}_m(k_r a) = \pm\frac{k_2}{\tau_2}\hat{K}_m(\tau_2 a) \tag{12}$$

where $\hat{J}_m(k_r a) = \frac{J'_m(k_r a)}{J_m(k_r a)}$, $\hat{K}_m(\tau_2 a) = \frac{K'_m(\tau_2 a)}{K_m(\tau_2 a)}$.

Energy flux along the z-axis in the waveguides is defined by

$$S_z = \frac{1}{2}\mathrm{Re}(\mathbf{E} \times \mathbf{H}^*) \cdot \hat{\mathbf{z}} = \frac{1}{2}\mathrm{Re}(E_r H_\varphi^* - E_\varphi H_r^*) \tag{13}$$

Energy flux in the core and cladding can be derived from above formulas:

$$S_{z1} = \frac{|A_m|^2 - |B_m|^2}{4\eta_1 k_r^2}\left[(\kappa k_0 + \beta)^2 J_{m+1}^2(k_r r) - (\kappa k_0 - \beta)^2 J_{m-1}^2(k_r r)\right] \tag{14a}$$

$$S_{z2} = \frac{C_m^2}{4\eta_2\tau_2^2}\left[(\beta + k_2)^2 K_{m+1}^2(\tau_2 r) - (\beta - k_2)^2 K_{m-1}^2(\tau_2 r)\right]$$
$$- \frac{D_m^2}{4\eta_2\tau_2^2}\left[(\beta - k_2)^2 K_{m+1}^2(\tau_2 r) - (\beta + k_2)^2 K_{m-1}^2(\tau_2 r)\right] \tag{14b}$$

Power is the integration of the energy flux:

$$P_1 = \int_0^{2\pi}\int_0^a r S_{z1} dr d\varphi = 2\pi\int_0^a r S_{z1} dr \tag{15a}$$

$$P_2 = \int_0^{2\pi}\int_a^\infty r S_{z2} dr d\varphi = 2\pi\int_a^\infty r S_{z2} dr \tag{15b}$$

Using the integration formulas of Bessel functions:

$$\int_0^a r J_n^2(k_r r) dr = \frac{a^2}{2}\left[J_n^2(k_r a) - J_{n-1}(k_r a)J_{n+1}(k_r a)\right],$$

$$\int_a^\infty r K_n^2(\tau_2 r) dr = -\frac{a^2}{2}\left[K_n^2(\tau_2 a) - K_{n-1}(\tau_2 a)K_{n+1}(\tau_2 a)\right];$$

We obtain the power in the core and cladding:

$$P_1 = \frac{\pi a^2(|A_m|^2 - |B_m|^2)}{4\eta_1 k_r^2} \left\{ (\kappa k_0 + \beta)^2 [J_{m+1}^2(k_r r) - J_m(k_r r) J_{m+2}(k_r r)] \right.$$
$$\left. - (\kappa k_0 - \beta)^2 [J_{m-1}^2(k_r r) - J_m(k_r r) J_{m-2}(k_r r)] \right\} \tag{16a}$$

$$P_2 = \frac{\pi a^2 C_m}{4\eta_2 \tau_2^2} \left\{ (\beta + k_2)^2 [K_m(\tau_2 a) K_{m+2}(\tau_2 a) - K_{m+1}^2(\tau_2 a)] \right.$$
$$\left. - (\beta - k_2)^2 [K_m(\tau_2 a) K_{m-2}(\tau_2 a) - K_{m-1}^2(\tau_2 a)] \right\}$$
$$- \frac{\pi a^2 D_m}{4\eta_2 \tau_2^2} \left\{ (\beta - k_2)^2 [K_m(\tau_2 a) K_{m+2}(\tau_2 a) - K_{m+1}^2(\tau_2 a)] \right.$$
$$\left. - (\beta + k_2)^2 [K_m(\tau_2 a) K_{m-2}(\tau_2 a) - K_{m-1}^2(\tau_2 a)] \right\} \tag{16b}$$

The normalized power is defined as

$$P = \frac{P_1 + P_2}{|P_1| + |P_2|} \tag{17}$$

3. NUMERICAL RESULTS AND DISCUSSION

We assume the cladding is air ($\varepsilon_2 = \varepsilon_0$, $\mu_2 = \mu_0$), the wave impedance of the chiral nihility metamaterial $\eta_1 = \eta_0$, and the chirality parameter $\kappa = 2.0$. We solve the dispersion Equation (12) for minus sign in the right side of Equation (12). Figs. 2(a) and (b) show the normalized
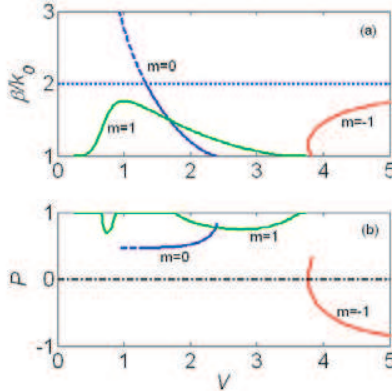
Figure 2. Lower-order ($m = 0$, $+1$, -1) modes in the chiral nihility fiber with the chirality parameter $\kappa = 2.0$ and air cladding. (a) Normalized propagation constants β/k_0. (b) Normalized power P.

propagation constants β/k_0 and their corresponding normalized power P versus normalized frequency V ($V = k_0 a \sqrt{\kappa^2 - n_2^2}$) for lower-order ($m = 0, +1, -1$) modes in the chiral nihility fiber. Here we use normalized frequency V (not frequency) because the chiral nihility metamaterial occurs only at certain frequency. For $m = 0$, surface mode solution (dashed curve) exist below the normalized frequency 1.332, it connects to guided mode (solid curve) at critical point 1.332, which is cross point of dotted line (corresponds to effective index of the chiral nihility fiber core equals to 2) and solid or dashed curves. The dispersion curve of $m = 0$ has negative slope, i.e., β/k_0 increases with V decreases from normalized cutoff frequency $V_c = 2.405$, which is the first root of $J_0(V_c) = 0$. It is found from computation that the power in the core and cladding are negative and positive, respectively. Its normalized power is positive and decreases as V decreases and becomes almost constant in the surface mode region. It indicates that the power $|P_1|$ in the core is smaller than the power P_2 in the cladding. The normalized propagation constants β/k_0 are different for different sign of m, i.e., $m = +1, -1$ guided modes have different propagation constants and different cutoff frequencies. For $m = -1$, the dispersion curve is bent, it has negative slope and positive slope. Below normalized cutoff frequency $V_c = 3.832$, which is the second root of $J_1(V_c) = 0$, there are two solution of β/k_0 for a fixed frequency. β/k_0 increases as V decreases from 3.832 to lowest limiting frequency or really cutoff frequency 3.768, and then β/k_0 increase as V increases from 3.768. Its power is positive for lower branch curve and negative for upper branch curve. For lower branch curve, P decreases to 0 as V decreases from 3.832 to lowest limiting frequency 3.768. For upper branch curve, P decreases from 0 to -1 as V increases from lowest limiting frequency
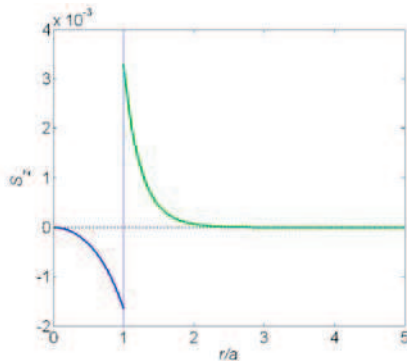
Figure 3. Energy flux S_z at $V = 1$ for $m = 0$ surface mode.
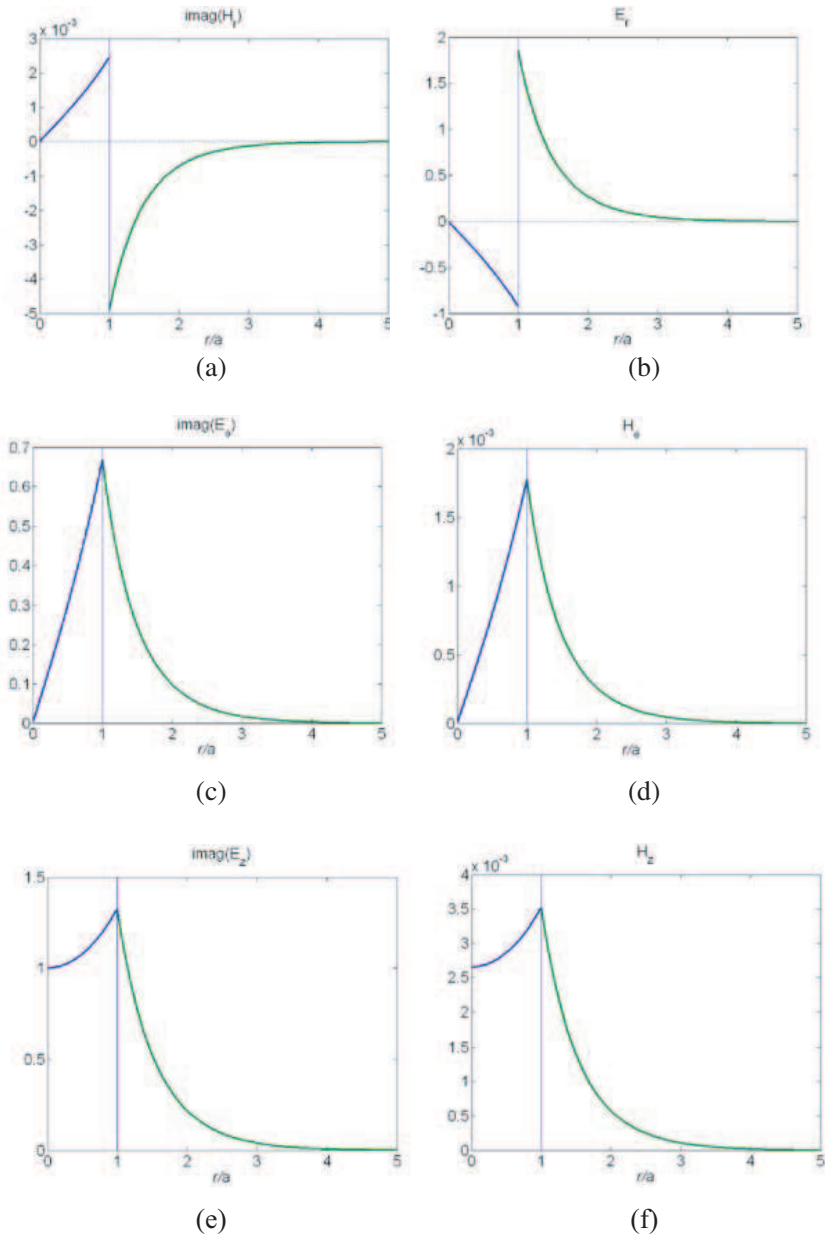
Figure 4. Amplitudes of electromagnetic field components at $V = 1$ for $m = 0$ surface mode.

3.768. It is interesting to note that the power P at lowest limiting frequency 3.768 equals to zero, corresponding to zero group velocity. It implies that at this point, the waveguide can not propagate energy. Waves with this feature are of great practical interest for optical communication and data storage applications [15]. For $m = 1$, guided mode exists in the region of between two normalized cutoff frequencies $V_c = 0$ and 3.832, which are the first and second roots of $J_1(V_c) = 0$. Its β/k_0 increases firstly and then decreases as V increases. This abnormal dispersion characteristic has not been found in chiral nihility planar waveguides [46] and in previous NIM circular waveguides [20–24]. Its normalized power is also positive. It is very interesting to note that at some region, its normalized power equals to 1. It means that the power in the chiral nihility fiber core is also positive. This phenomenon has been found in NIM circular waveguide [22]. Another interesting phenomena is intersection of curves of $m = 0$ and $m = 1$ guided mode in Fig. 2. It means these modes have same propagation constant (mode matching or perfect phase matching) at crossing point $V = 1.695$. Mode matching can be applied for polarization-intensive, efficient fiber-to-planar waveguide coupling, and improvement of mode conversion efficiency [20].

Figures 3 and 4 show the energy flux S_z and the amplitudes of electromagnetic field components at normalized frequency $V = 1$ for $m = 0$ surface mode. The energy flux S_z in the cladding is positive and S_z in the core is negative (Fig. 3). It indicates that the energy flux of surface mode is in opposite directions in the core and cladding. The total power is always positive so it is a forward wave. These results hold true for $m = 0$ guided mode. All electromagnetic field components of the surface mode are decay exponentially from the interface between
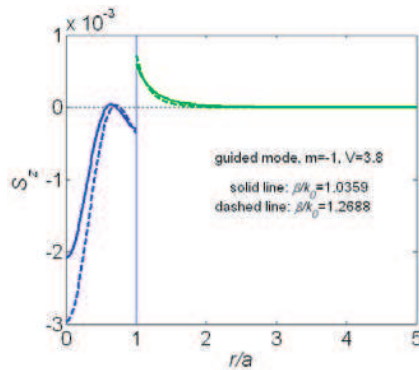
Figure 5. Energy flux S_z at $V = 3.8$ for $m = -1$ guided mode.

the core and cladding (Fig. 4). Transversal electromagnetic fields of $m = 0$ guided mode are also similar as in Fig. 4.

Figure 5 shows the energy flux S_z at normalized frequency $V = 3.8$ for $m = -1$ guided mode. There are two normalized propagation constants β/k_0 at $V = 3.8$. Solid and dashed line corresponds to smaller and larger β/k_0. The two curves of the energy flux S_z are similar. However, their values are different. The energy flux S_z is negative in the most core region and positive in the cladding. For smaller propagation constant $\beta/k_0 = 1.0359$, the absolute power $|P_1|$ in the core is smaller than the power P_2 in the cladding, thus the total power is positive. For larger propagation constant $\beta/k_0 = 1.2688$, the absolute power $|P_1|$ in the core is larger than the power P_2 in the cladding, thus the total power is negative (see Fig. 2(b)).

Figure 6 shows the energy flux S_z at different normalized frequency V for $m = 1$ guided mode. It can be seen from Figs. 3, 5, and 6, the energy flux change sign at the interface between the core and cladding, which has been known in NIM waveguides, including slab [14], grounded slab [19], and fiber [20]. However, for $m = 1$ guided mode, besides the interface, the energy flux S_z also changes sign in the cladding (air) for smaller V (Figs. 6(a) and (b)) and in the chiral nihility fiber core for larger V (Figs. 6(d), (e), and (f)). For $V = 0.5, 1.0$, the energy flux S_z is positive in the core. However, in the cladding, S_z is negative near the interface and positive away from the interface. It is an exotic feature has not been previously found in NIM waveguides. For $V = 1.26$, the energy flux S_z are positive in the core and decreases from maximum at the center to zero at the interface, and the location of varying-sign energy flux in the cladding shifts to the interface (Fig. 6(c)). For $V = 1.5, 2.5, 3.5$, the energy flux S_z are positive close to center and negative close to the interface in the core, S_z are all positive and decay rapidly from the interface in the cladding. This phenomenon that the energy flux changes sign within the NIM region has been found in Ref. [22].

The power is the integration of energy flux. It is found that the power both in the core and cladding are positive for $V = 0.5, 1.0, 1.26, 1.5$, thus the normalized power equals to one. For $V = 2.5, 3.5$, the power in the core is negative, however, its absolute value $|P_1|$ is smaller than positive power P_2 in the cladding, thus the total power is positive, the normalized power is less than one (see Fig. 2(b)).

In the above numerical results and discussion, we have assumed $\eta_1 = \eta_0$ and $\kappa = 2.0$. For different values of η_1, it is found that although the values of energy flux S_z are different, the relationship of S_z in the core and cladding does not change, and the power P is the same as those for $\eta_1 = \eta_0$. For different chirality parameter ($\kappa > 1$), the exotic

(a) $V=0.5$, $\beta / k_0 = 1.0667$;

(b) $V=1.0$, $\beta / k_0 = 1.7585$;

(c) $V=1.26$, $\beta / k_0 = 1.6919$;

(d) $V=1.5$, $\beta / k_0 = 1.5822$;

(e) $V=2.5$, $\beta / k_0 = 1.1873$;

(f) $V=3.5$, $\beta / k_0 = 1.0040$.
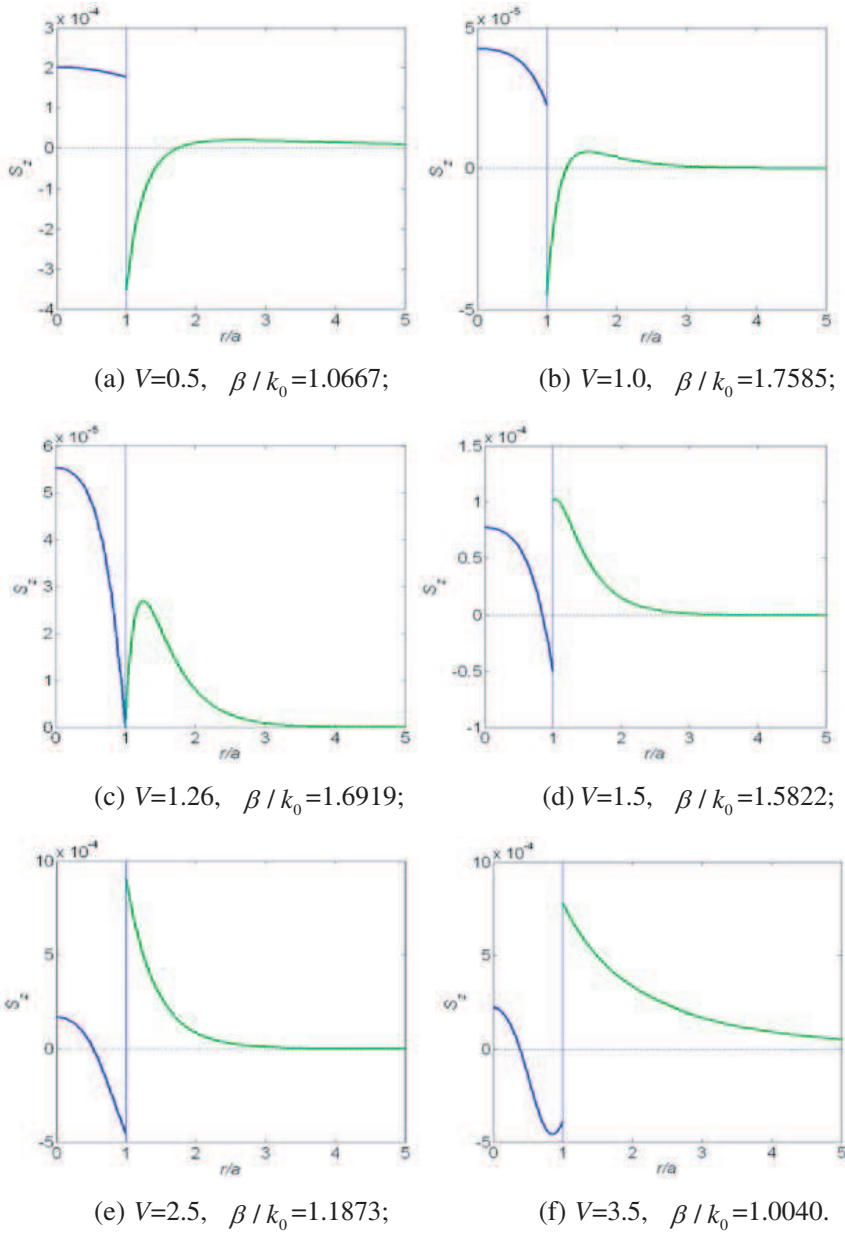
Figure 6. Energy flux S_z at different V for $m = 1$ guided mode.

power propagation is also found, i.e., for $m = 1$ mode, the energy flux S_z is negative near the interface and positive away from the interface for smaller V, although the surface mode occurs in some region of V for smaller chirality parameter [52].

In addition, for plus sign in the right side of Equation (12), no unusual phenomenon of power propagation of guided modes can be found and the numerical results are not shown in this paper. The difference between the mode of the positive and the negative sign in Equation (12) can be understood from the fact that the chiral nihility behaves as a medium with a single bulk wavenumber $k_+ = \kappa k_0$ (conventional material) for positive sign, and it behaves as having a single bulk wavenumber $k_- = -\kappa k_0$ (negative index material) for negative sign [49].

4. CONCLUSION

The characteristics of power propagation of guided modes in the chiral nihility fiber which is consists of a chiral nihility metamaterial core with an achiral cladding have been investigated theoretically. The formulas of electromagnetic fields in the core and cladding for guided modes are presented in detail. The dispersion equations, energy flux and power of guided modes in the chiral nihility fiber are obtained. The numerical results are given and discussed. There exists $m = 1$ guided mode in the region of between two normalized cutoff frequencies $V_c = 0$ and 3.832. This abnormal dispersion characteristic has not been found in chiral nihility planar waveguides and in previous NIM circular waveguides. For $m = 1$ guided mode, besides the interface between the core and cladding, energy flux also changes sign in the cladding for smaller V. It is an exotic feature which has not been found in NIM waveguides. It is very interesting to note that the curves of guided mode will intersect with each other. The results presented here will helpful for potential applications in novel fiber devices.

REFERENCES

1. Smith, D. R., W. J. Padilla, D. C. Vier, S. C. Nemat-Nasser, and S. Schultz, "Composite medium with simultaneously negative

permeability and permittivity," *Phys. Rev. Lett.*, Vol. 84, No. 18, 8184–4187, 2000.

2. Shelby, R. A., D. R. Smith, and S. Shultz, "Experimental verification of a negative index of refraction," *Science*, Vol. 292, 77–79, 2001.

3. Chen, H., B. I. Wu, and J. A. Kong, "Review of electromagnetic theory in left-handed materials," *Journal of Electromagnetic Waves and Applications*, Vol. 20, No. 15, 2137–2151, 2006.

4. Grzegorczyk, T. M. and J. A. Kong, "Review of left-handed metamaterials: Evolution from theoretical and numerical studies to potential applications," *Journal of Electromagnetic Waves and Applications*, Vol. 20, No. 14, 2053–2064, 2006.

5. Tang, W. X., H. Zhao, X. Zhou, J. Y. Chin, and T. J. Cui, "Negative index material composed of meander line and SRRs," *Progress In Electromagnetics Research B*, Vol. 8, 103–114, 2008.

6. Wang, J., S. Qu, H. Ma, J. Hu, Y. Yang, X. Wu, Z. Xu, and M. Hao, "A dielectric resonator-based route to left-handed metamaterials," *Progress In Electromagnetics Research B*, Vol. 13, 133–150, 2009.

7. Veselago, V. G., "The electrodynamics of substances with simultaneously negative values of ε and μ," *Sov. Phys. Usp.*, Vol. 10, No. 4, 509–514, 1968.

8. Pendry, J. B., "Negative refraction makes a perfect lens," *Phys. Rev. Lett.*, Vol. 85, No. 18, 3966–3969, 2000.

9. Schurig, D., J. J. Mock, B. J. Justice, S. A. Cummer, J. B. Pendry, A. F. Starr, and D. R. Smith, "Metamaterial electromagnetic cloak at microwave frequencies," *Science*, Vol. 314, 977–980, 2006.

10. Tsakmakidis, K. L., A. D. Boardman, and O. Hess, "'Trapped rainbow' storage of light in metamaterials," *Nature,* Vol. 450, 397–401, 2007.

11. Li, Z. and T. J. Cui, "Novel waveguide directional couplers using left-handed materials," *Journal of Electromagnetic Waves and Applications*, Vol. 21, No. 8, 1053–1062, 2007.

12. Hsu, H. T. and C. J. Wu, "Design rules for a Fabry-Perot narrow band transmission filter containing a metamaterial negative-index defect," *Progress In Electromagnetics Research Letters*, Vol. 9, 101–107, 2009.

13. Lindell, I. V. and S. Ilvonen, "Waves in a slab of uniaxial BW medium," *Journal of Electromagnetic Waves and Applications*, Vol. 16, No. 3, 303–318, 2002.

14. Shadrivov, I. V., A. A. Sukhorukov, and Y. S. Kivshar, "Guided

modes in negative-refractive-index waveguides," *Phys. Rev. E*, Vol. 67, 057602, 2003.

15. Tsakmakidis, K. L., C. Hermann, A. Klaedtke, C. Jamois, and O. Hess, "Surface plasmon polaritons in generalized slab heterostructures with negative permittivity and permeability," *Phys. Rev. B*, Vol. 73, 085104, 2006.

16. Wang, Z. J. and J. F. Dong, "Analysis of guided modes in asymmetric left-handed slab waveguides," *Progress In Electromagnetics Research*, PIER 62, 203–215, 2006.

17. Mahmoud, S. F. and A. J. Viitanen, "Surface wave character on a slab of metamaterial with negative permittivity and permeability," *Progress In Electromagnetics Research*, PIER 51, 127–137, 2005.

18. Li, C., Q. Sui, and F. Li, "Complex guided wave solutions of grounded dielectric slab made of metamaterials," *Progress In Electromagnetics Research*, PIER 51, 187–195, 2005.

19. Shu, W. and J. M. Song, "Complete mode spectrum of a grounded dielectric slab with double negative metamaterials," *Progress In Electromagnetics Research*, PIER 65, 103–123, 2006.

20. Novitsky, A. V. and L. M. Barkovsky, "Guided modes in negative-refractive-index fibres," *J. Opt. A: Pure Appl. Opt.*, Vol. 7, S51–S56, 2005.

21. Cory, H. and T. Blum, "Surface-wave propagation along a metamaterial cylinder guide," *Microwave Opt. Technol. Lett.*, Vol. 44, No. 1, 31–35, 2005.

22. Kim, K. Y., J. H. Lee, Y. K. Cho, and H. S. Tae, "Electromagnetic wave propagation through doubly dispersive subwavelength metamaterial hole," *Optics Express*, Vol. 13, No. 10, 3653–3665, 2005.

23. Kim, K. Y., "Fundamental guided electromagnetic dispersion characteristics in lossless dispersive metamaterial clad circular air-hole waveguides," *J. Opt. A, Pure Appl. Opt.*, Vol. 9, No. 11, 1062–1069, 2007.

24. Shen, L. F. and Z. H. Wang, "Guided modes in fiber with left-handed materials," *J. Opt. Soc. Am. A*, Vol. 26, No. 4, 754–759, 2009.

25. Tretyakov, S., I. Nefedov, A. Sihvola, S. Maslovski, and C. Simovski, "Waves and energy in chiral nihility," *Journal of Electromagnetic Waves and Applications*, Vol. 17, No. 5, 695–706, 2003.

26. Pendry, J. B., "A chiral route to negative refraction," *Science*, Vol. 306, 1353–1355, 2004.

27. Tretyakov, S., A. Sihvola, and L. Jylhä, "Backward-wave regime and negative refraction in chiral composites," *Photonics and Nanostructures*, Vol. 3, No. 2–3, 107–115, 2005.

28. Faryad, M. and Q. A. Naqvi, "Cylindrical reflector in chiral medium supporting simultaneously positive phase velocity and negative phase velocity," *Journal of Electromagnetic Waves and Applications*, Vol. 22, No. 4, 563–572, 2008.

29. Monzon, C. and D. W. Forester, "Negative refraction and focusing of circularly polarized waves in optically active media," *Phys. Rev. Lett.*, Vol. 95, 123904, 2005.

30. Jin, Y. and S. He, "Focusing by a slab of chiral medium," *Optics Express*, Vol. 13, No. 13, 4974–4979, 2005.

31. Plum, E., J. Zhou, J. Dong, V. A. Fedotov, T. Koschny, C. M. Soukoulis, and N. I. Zheludev, "Metamaterial with negative index due to chirality," *Phys. Rev. B*, Vol. 79, 035407, 2009.

32. Zhou, J., J. Dong, B. Wang, T. Koschny, M. Kafesaki, and C. M. Soukoulis, "Negative refractive index due to chirality," *Phys. Rev. B*, Vol. 79, 121104, 2009.

33. Wang, B., J. Zhou, T. Koschny, and C. M. Soukoulis, "Nonplanar chiral metamaterials with negative index," *Appl. Phys. Lett.*, Vol. 94, 151112, 2009.

34. Zhang, S., Y. Park, J. Li, X. Lu, W. Zhang, and X. Zhang, "Negative refractive index in chiral metamaterials," *Phys. Rev. Lett.*, Vol. 102, 023901, 2009.

35. Wiltshire, M. C. K., J. B. Pendry, and J. V. Hajnal, "Chiral Swiss rolls show a negative refractive index," *J. Phys.: Condens. Matter*, Vol. 21, No. 29, 292201, 2009.

36. Dong, J., J. Zhou, T. Koschny, and C. M. Soukoulis, "Bi-layer cross chiral structure with strong optical activity and negative refractive index," *Optics Express*, Vol. 17, No. 16, 14172–14179, 2009.

37. Jin, Y., J. He, and S. He, "Surface polaritons and slow propagation related to chiral media supporting backward waves," *Phys. Lett. A*, Vol. 351, No. 4–5, 354–358, 2006.

38. Zhang, C. and T. J. Cui, "Chiral planar waveguide for guiding single-mode backward wave," *Opt. Commun.*, Vol. 280, No. 2, 359–363, 2007.

39. Dong, J. F., "Surface wave modes in chiral negative refraction grounded slab waveguides," *Progress In Electromagnetics Research*, PIER 95, 153–166, 2009.

40. Dong, J. F., Z. J. Wang, L. L. Wang, and B. Liu. "Novel char-

acteristics of guided modes in chiral negative refraction waveguides," *Proceedings of International Symposium on Biophotonics, Nanophotonics and Metamaterials, Metamaterials 2006*, 517–520, Oct. 2006.

41. Naqvi, Q. A., "Fractional dual interface in chiral nihility medium," *Progress In Electromagnetics Research Letters*, Vol. 8, 135–142, 2009.

42. Cheng, Q. and C. Zhang, "Waves in planar waveguide containing chiral nihility metamaterial," *Opt. Commun.*, Vol. 276, No. 2, 317–321, 2007.

43. Naqvi, Q. A., "Planar slab of chiral nihility metamaterial backed by fractional dual/PEMC interface," *Progress In Electromagnetics Research*, PIER 85, 381–391, 2008.

44. Naqvi, Q. A., "Fractional dual solutions in grounded chiral nihility slab and their effect on outside field," *Journal of Electromagnetic Waves and Applications*, Vol. 23, No. 5–6, 773–784, 2009.

45. Illahi, A. and Q. A. Naqvi, "Study of focusing of electromagnetic waves reflected by a PEMC backed chiral nihility reflector using Maslov's method," *Journal of Electromagnetic Waves and Applications*, Vol. 23, No. 7, 863–873, 2009.

46. Dong, J. F. and C. Xu, "Characteristics of guided modes in planar chiral nihility metamaterial waveguides," *Progress In Electromagnetics Research B*, Vol. 14, 107–126, 2009.

47. Dong, J. F. and C. Xu, "Surface polaritons in planar chiral nihility metamaterial waveguides," *Opt. Commun.*, Vol. 282, No. 19, 3899–3904, 2009.

48. Qiu, R. C. and I.-T. Lu, "Guided waves in chiral optical fibers," *J. Opt. Soc. Am. A*, Vol. 11, No. 12, 3212–3219, 1994.

49. Mahmoud, S. F., "Guided modes on open chirowaveguides," *IEEE Trans. Microwave Theory Tech.*, Vol. 43, No. 1, 205–209, 1995.

50. Nair, A. and P. K. Choudhury, "On the analysis of field patterns in chirofibers," *Journal of Electromagnetic Waves and Applications*, Vol. 21, No. 15, 2277–2286, 2007.

51. Dong, J. F., W. D. Tao, and J. Xu, "Optical power characteristics of guided modes in a double cladding chiral optical fiber," *Acta Photonica Sinica*, Vol. 36, No. 6, 1044–1049, 2007.

52. Dong, J. F., "Guided and surface modes in chiral nihility fiber," *Opt. Commun.*, 2009, doi: 10.1016/j.optcom.2009.10.086.